

## Visualization of natural convection heat transfer on a sphere with various contact points

M. S. Park, J. W. Han and B. J. Chung\*

Department of Nuclear Engineering, Kyung Hee University

#1732 Deogyong-daero, Giheung-gu, Yongin-si, Gyeonggi-do, 17104, Republic of Korea

\*Corresponding author: bjchung@khu.ac.kr

\***Keywords** : Packed bed, Natural convection heat transfer, Analogy, Heat transfer visualization

### 1. Introduction

Convective heat transfer in a packed bed has been applied in various engineering applications, such as the pebble bed nuclear reactors and heat exchangers due to its large heat transfer area and complex flow passage [1].

This work stemmed from a curiosity why the natural convection heat transfers of a single sphere in an open pool and in an unheated packed bed show similar values. In a randomly stacked pebble bed, the flow paths become complex, leading to complicated flow phenomena around the pebbles, which in turn affect the heat transfer. Numerous investigations were made so far on the heat transfer of packed beds. However, most of them focused on overall heat transfer rather than the heat transfer among individual pebbles [1–3]. The heat transfer can vary depending on the contacting conditions under which each sphere makes contact with one another. Therefore, analyzing the heat transfer between individual pebbles can contribute to a better understanding of the heat transfer mechanisms within packed bed structures.

This study investigated the effect of contact position on the natural convection heat transfer around a single sphere. The mass transfer experimental method was employed based on the analogy between heat and mass transfers. Copper electroplating system was adopted, and copper sulfate-sulfuric acid ( $\text{CuSO}_4\text{-H}_2\text{SO}_4$ ) was used as working fluid. By employing this experimental technique, heat transfer was visualized via the plating pattern. The sphere diameter was 0.0158 m and 0.04m, which corresponds to  $Ra_d$  of  $1.83 \times 10^7$  and  $5.43 \times 10^9$ , respectively. The  $Sc$ , which corresponds to  $Pr$ , was 2,014.

### 2. Background theories

#### 2.1 Natural convection heat transfer on a sphere

Figure 1 illustrates the variation in local heat transfer as a function of Rayleigh number ( $Ra$ ) and contact angle ( $\theta$ ) on a sphere. Schutz conducted measurements of local heat transfer at various points on a single sphere using a copper plating experimental technique [4]. As the contact angle increase, heat transfer initially decreases and then increases as the transition to turbulence regime begins. With increasing the sphere diameter, the heat transfer was enhanced, but the variation trend was similar. Furthermore, the onset of the turbulence regime occurred at lower contact angles as the sphere diameter increased.

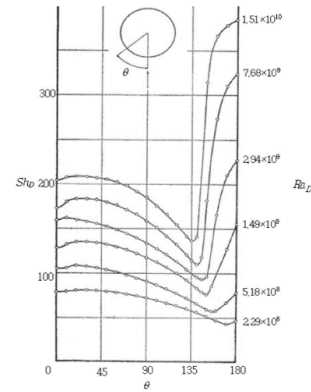


Fig. 1. Local mass transfer on spheres for different  $Ra_D$  [5].

#### 2.2 Natural convection heat transfer in packed bed

Lee et al. conducted a comparative analysis of heat transfer experimental results for a single heated sphere within an unheated packed bed and an open channel [2]. Figure 2 illustrates the development of the natural convection boundary layer in both the open channel and the packed bed geometry. Within the packed bed, the boundary layer is broken by dimples formed due to the contact between spheres. Although these contacts affect the boundary layer's development, the measured heat transfer in the packed bed and open pool remain same. This result suggests compensating mechanism that the contact-induced thin boundary layer thickness, which could potentially increase heat transfer, are offset by heat transfer decrease due to the decreased heat transfer area at the point of contact [2].

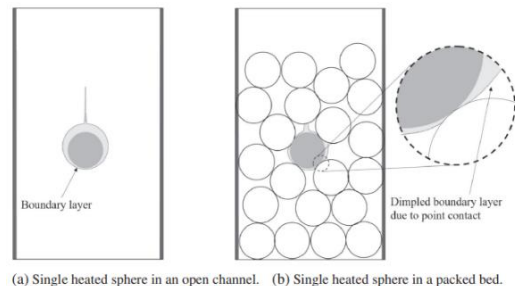


Fig. 2. Local mass transfer on spheres for different  $Ra_d$  [2].

#### 2.3 Visualization of flow separation

Kitamura et al. visualized the natural convection flow around a sphere through mass transfer experiments [6]. Figure 3 depicts how the flow develops around a single.

The lift-up point is characterized by the thickened boundary layer enough to detach and ascend from the sphere by buoyancy. This point serves as a criterion for distinguishing between laminar and turbulent flows. It was observed that with an increase in the Rayleigh number ( $Ra$ ), the lift-up point forms further upstream [6].

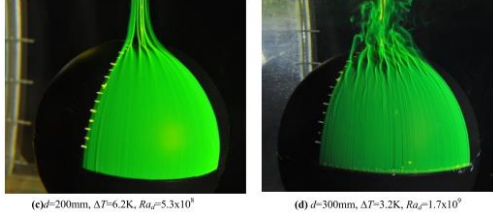


Fig. 3. Visualizations of natural convective flows induced around spheres [6].

### 3. Experimental setup

#### 3.1 Methodology

Mass transfer experiment was performed by replacing the heat transfer experiment based on the analogy between heat transfer and mass transfer. In order to achieve high  $Ra_d$  efficiently,  $\text{CuSO}_4\text{-H}_2\text{SO}_4$  electroplating system was adopted as the mass transfer system. The transfer of copper ions to the cathode causes a concentration difference of copper ions around the anode, resulting in a difference in density. Therefore, transfer of copper ions from the anode to the cathode corresponds to natural convection heat transfer [7].

The mass transfer coefficient ( $h_m$ ) may be calculated by measuring a current value from an experiment by Equation (1).  $I_{lim}$  is limiting current density and  $C_b$  is the bulk concentration, corresponding heat flux and temperature difference, respectively. Further details of the technique is explained in a previous study [8].

$$h_m = \frac{(1-t_n)I_{lim}}{nFC_b} \quad (1)$$

#### 3.2 Test matrix and experimental apparatus

Table 1 lists the test matrix for the experiments. The sphere diameter was 0.0158 m and 0.04 m, which corresponds to  $Ra_d$  of  $1.83 \times 10^7$  and  $5.43 \times 10^9$ , respectively. The  $Sc$ , which corresponds to  $Pr$ , was 2,014. Contact point ( $\theta$ ) between spheres are 0, 30, 60, 90, 120, 135, 150, 180. Copper sulfate-sulfuric acid ( $\text{CuSO}_4\text{-H}_2\text{SO}_4$ ) of 0.05 M and 1.5 M, was used as working fluid.

Table 1. Test matrix

$Sc$	$d (\times 10^{-2}\text{m})$	$Ra_d$	Contact angle ( $^\circ$ )
2,014	1.58	$3.35 \times 10^8$	0
			30
			60
			90
			120
	4	$5.43 \times 10^9$	135
			150
			180

Figure 4 shows the experimental circuit and apparatus. Cathode copper sphere is connected to an insulated copper rod and contained in an acrylic container filled with a  $\text{CuSO}_4\text{-H}_2\text{SO}_4$  solution. The electrical power was supplied via a power source (Vüpower K1810), and the electrical current was recorded using the DAQ (NI 9227).

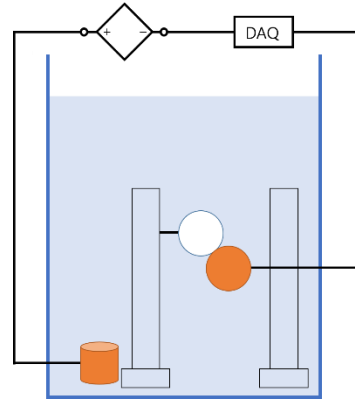


Fig. 4. Electric circuit and experimental apparatus.

### 4. Results and discussion

#### 4.1 Comparison with existing correlation for single sphere

Figure 5 shows a comparison of present experimental results with existing heat transfer correlations for a single sphere in an open pool. It indicates that our results for both the 15.8 mm and 40 mm spheres closely matched the results of existing studies.

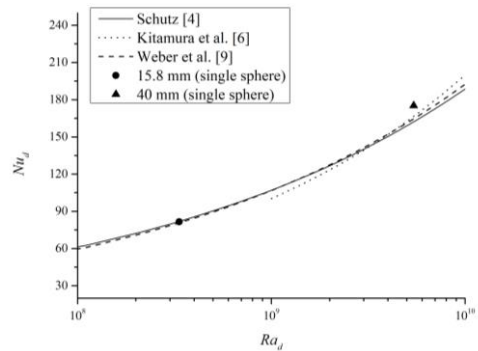


Fig. 5. Comparison test results with correlations.

#### 4.2 Influence of contact point on natural convective heat transfer on sphere

Figure 6 shows measured  $Nu_d$  of the sphere according to the contact angle. The presence of a contact point showed minimal difference in the  $Nu_d$  value. These minimal differences result from compensatory effects: the enhancement of heat transfer due to a thinned boundary layer and the weakening of heat transfer due to a reduced heat transfer area.

In the case of the 0.04 m sphere contacted at 180 degrees, the  $Nu_d$  was decreased compared to other cases. This is because at the top of the sphere, which corresponds to the turbulent region beyond the lift-up point, there is no area for the redevelopment of the boundary layer to compensate for heat transfer loss. As a result, only a reduction in the heat transfer area occurs without any enhancement in heat transfer by the redevelopment of the boundary layer. However, for the 0.0158 m sphere, the top of the sphere still had areas where the laminar region was developing, indicating that the enhancement in heat transfer due to the redevelopment of the boundary layer acted to compensate for heat transfer loss.

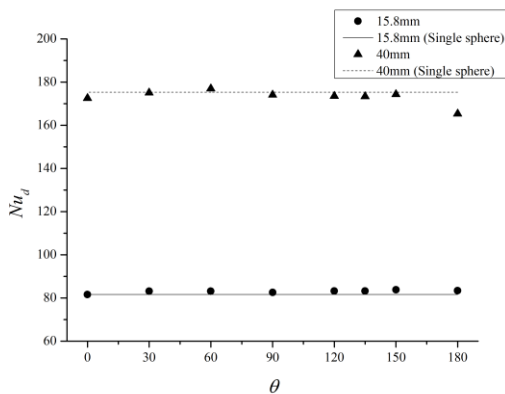


Fig. 6.  $Nu_d$  variations according to contact angle

#### 4.3 Visualization of heat transfer

Figure 7 compares electroplating patterns according to the size of the sphere and the contact angle. At the sphere's bottom, within the laminar region, contact points lead to intensified plating beyond the contact point, signifying improved heat transfer through boundary layer redevelopment. This suggests that the reduction in heat transfer area from contact with an unheated sphere is offset by the boundary layer's regeneration. At the top of the sphere, the area of contact affects the plating intensity differently, depending on whether the flow is laminar, transitioning, or turbulent. In the laminar and transition regions, we observe patterns indicating enhanced heat transfer or bending corresponding to the transition area. However, at 180 degrees, where the boundary layer cannot redevelop, heat transfer degradation occurs without compensation, as the dominance of the contact point area leads to a more

significant reduction in heat transfer than any potential gains from boundary layer redevelopment.

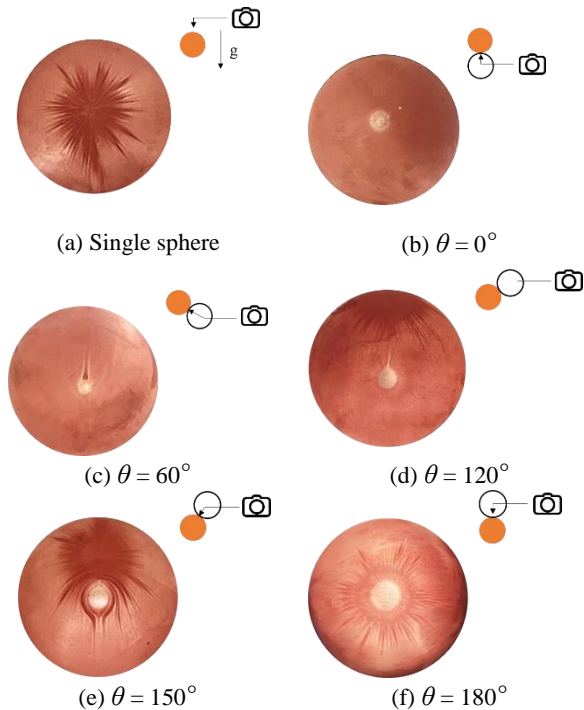


Fig. 7 Visualization of heat transfer at  $d = 40$  mm.

#### 5. Conclusions

The influence of the contact point on the natural convection heat transfer of a sphere was investigated. By utilizing a mass transfer experimental methodology, heat transfer was visualized and analyzed according to the flow regime. The heat transfer in conditions where the sphere was in contact was found to be similar to that of a sphere without contact, due to a compensation between enhancement and impairment effects on heat transfer. However, the electroplating patterns exhibited different trends based on the flow regime and the position of contact. The authors expect that these findings will provide fundamental insights for a better understanding of heat transfer in packed beds, which involve complex contact conditions.

#### ACKNOWLEDGEMENT

This study was sponsored by the Ministry of Science and ICT (MSIT) and was supported by nuclear Research & Development program grant funded by the National Research Foundation (NRF) (Grant codes 2020M2D2A1A02065563).

#### REFERENCES

- [1] H.H. Ahn, J.Y. Moon and B.J. Chung, Anode influence on the electrochemical realization of packed bed heat transfer, Heat and Mass Transfer, Vol. 57 pp. 1685–1695, 2021.

- [2] D.Y. Lee, M. S. Chae, B. J. Chung, Natural convective heat transfer of heated packed beds, *International Communications in Heat and Mass Transfer*, Vol. 88 pp. 54–62, 2017.
- [3] H.H. Ahn, J.Y. Moon and B.J. Chung, Influences of sphere diameter and bed height on the natural convection heat transfer of packed beds, *International Journal of Heat and Mass Transfer*, Vol.194, 2022.
- [4] G. Schütz, Natural convection mass-transfer measurements on spheres and horizontal cylinders by electrochemical method. *International Journal of Heat and Mass Transfer*, Vol.6 pp. 873–879, 1963.
- [5] D.Y. Lee, B.J. Chung, Visualization of natural convection heat transfer on a sphere. *Heat and Mass Transfer*, Vol. 53 pp. 3613–3620, 2017.
- [6] K. Kitamura, A. Mitsuishi, T. Suzuki, T. Misumi, Fluid flow and heat transfer of high-Rayleigh-number natural convection around heated spheres, *International Journal of Heat and Mass Transfer*, Vol. 86 pp. 149–157, 2015.
- [7] H.H. Ahn, J.Y. Moon, D.H. Park, B.J. Chung, Natural convection heat transfer of the packed bed varying the bed height and sphere diameter, *Transactions of the Korean Nuclear Society Spring Meeting*, 2021.
- [8] H.K. Park, B.J. Chung, Mass transfer experiments for the heat load during in-vessel retention of Core melt, *Nucl. Eng Technol.*, Vol. 48 pp. 906–914, 2016.
- [9] M.E. Weber, P. Astrauskas, S. Petsalis S, Natural convection mass transfer to Nonspherical objects at high Rayleigh number, *The Canadian Journal of Chemical Engineering*, Vol. 62 pp. 68–72, 1984.